JGR Oceans

RESEARCH ARTICLE
10.1029/2025JC023763

The Roles of Kuroshio-Origin New and Regenerated Nutrients Over the East China Sea Shelf

C. C. Shi[1], Y. N. He[1], X. Y. Guo[2], S. D. Guan[3,4], L. N. Wang[5], L. Zhao[1,6], and J. Zhang[1,3,6]

[1]College of Marine and Environmental Sciences, Tianjin University of Science and Technology, Tianjin, China, [2]Center for Marine Environmental Studies, Ehime University, Matsuyama, Japan, [3]Key Laboratory of Ocean Observation and Information of Hainan Province, Sanya Oceanographic Institution, Ocean University of China, Sanya, China, [4]Sanya Oceanographic Laboratory, Sanya, China, [5]Tianjin Marine Center, Ministry of Natural Resources, Tianjin, China, [6]Key Laboratory of Marine Resource Chemistry and Food Technology (TUST), Ministry of Education, Tianjin, China

Key Points:

- The Kuroshio-origin new nutrients make up 72.8% of the total inventory
- New production supported by Kuroshio nutrients comprises 44.0% of primary production, and regenerated production comprises the rest
- A mismatch between new and export production is caused by offshore transport of regenerated nutrients from the shelf

Supporting Information:

Supporting Information may be found in the online version of this article.

Correspondence to:

J. Zhang,
zhangjing@tust.edu.cn

Citation:

Shi, C. C., He, Y. N., Guo, X. Y., Guan, S. D., Wang, L. N., Zhao, L., & Zhang, J. (2026). The roles of Kuroshio-origin new and regenerated nutrients over the East China Sea shelf. *Journal of Geophysical Research: Oceans*, *131*, e2025JC023763. https://doi.org/10.1029/2025JC023763

Received 18 NOV 2025
Accepted 12 APR 2026

Author Contributions:

Conceptualization: X. Y. Guo, L. Zhao, J. Zhang
Formal analysis: C. C. Shi
Investigation: S. D. Guan, L. N. Wang, L. Zhao
Methodology: L. Zhao
Resources: S. D. Guan, L. N. Wang
Supervision: J. Zhang
Validation: C. C. Shi
Visualization: C. C. Shi
Writing – original draft: C. C. Shi, Y. N. He
Writing – review & editing: X. Y. Guo, J. Zhang

Abstract The Kuroshio brings a large amount of nutrients into the East China Sea, making it the largest source of external nutrients. However, significant unknowns remain regarding how they support primary production and how these Kuroshio-intruded nutrients are regenerated in the East China Sea. A physical-biological coupled module and a nutrient tracking module were used to classify Kuroshio nutrients (including dissolved inorganic phosphorus and dissolved inorganic nitrogen (DIN)) into two types: new nutrients and regenerated nutrients. The spatiotemporal distributions of new and regenerated nutrients in the East China Sea shelf were examined, and the contributions of Kuroshio nutrients to the new and regenerated production on the East China Sea shelf were assessed. New production supported by new nutrients is mainly located in the outer shelf, while the regenerated production supported by regenerated nutrients can extend into the inner shelf. The new (regenerated) DIN makes up 72.8% (27.2%) of the total inventory of DIN from the Kuroshio over the East China Sea and the new (regenerated) production accounts for 44.0% (56.0%) of primary production using DIN from Kuroshio. The new and export productions supported by Kuroshio nutrients are not balanced in the ECS shelf. The difference between them is attributed to the offshore transport of the regenerated nutrients, which induces a part of the regenerated nutrients not used for the export production in the ECS shelf. Therefore, lateral transport of regenerated nutrients away from shelf seas can serve as a new process for understanding the mismatch of new and export production there.

Plain Language Summary A strong western boundary current, the Kuroshio, supplies most of the nutrients to the East China Sea. We studied how these nutrients fuel the growth of phytoplankton, which form the base of the ocean food web. We demonstrated that these nutrients can be separated into two types: "new" and "recycled." The new nutrients, which make up most of the supply, support about 40% of the primary production using the nutrients from Kuroshio, mainly in the deeper parts of the sea. Surprisingly, the recycled nutrients, despite being a smaller part of the total amount, can spread into coastal areas and support over half of the primary production using the nutrients from Kuroshio. We also found that the leaving of the recycled nutrients away from the shelf sea with ocean currents can explain the imbalance between the new primary production and export production in the shelf sea, which is important for understanding how ocean ecosystems work.

1. Introduction

The East China Sea (ECS) is a typical continental shelf in the northwest Pacific Ocean, with high primary productivity (Gong et al., 2003), and bears the intrusion of the Kuroshio Current (Wang, Dai, et al., 2016; Xu et al., 2018; Yang et al., 2012; Zhou et al., 2015). The Kuroshio is a strong western boundary current, with low nutrient concentrations in its surface waters but high concentrations in its subsurface waters (Guo et al., 2012). The Kuroshio intrudes into the ECS continental shelf across the 200-m isobath (Lee & Takeshi, 2007). The annual average volume transport of Kuroshio intrusion across the shelf into the ECS can reach 1.46 Sv (Guo et al., 2006), which is the largest in autumn and the smallest in summer (Guo et al., 2006; Teague et al., 2003; Wu et al., 2014). The Kuroshio intrusion on the ECS mainly occurs in the northeast of Taiwan, the central shelf, and southwest of Kyushu (Zhang et al., 2017). Therefore, through water exchange between the Kuroshio and the ECS, the Kuroshio becomes the primary source of oceanic nutrients for the ECS shelf (Zhang et al., 2007). However, only the nutrients supporting primary production have an impact on the marine ecosystem. The dissolved inorganic

nitrogen (DIN) input flux originating from the Kuroshio accounts for over 70% of the total input into the ECS, but the primary production it supports only accounts for 50% of that in the ECS (Zhang et al., 2019).

Primary production can be separated into two parts: regenerated production and new production. Regenerated production utilizes recycled nutrients within the euphotic zone, which phytoplankton can use multiple times. In contrast, new production utilizes nutrients supplied from outside the euphotic zone, which phytoplankton can only use once. Thus, Dugdale and Goering (1967) defined regenerated nutrients (primarily ammonium) and new nutrients (primarily nitrate) in the form of nitrogen. New nutrients in the open ocean originate from the atmosphere and below the euphotic zone. In the shelf seas, new nutrients originate from rivers, atmosphere and oceanic inputs.

It is also important to note that nutrients located beneath the euphotic layer in shelf seas are not "new" and are easily replenished to the upper layer. This is in contrast to the open ocean, where nutrients can be isolated from the upper layer for a long period of time (Simpson & Sharples, 2012).

Some of these new nutrients may leave the ecosystem directly without ever being utilized, such as nutrients from the Kuroshio intruding into the ECS, which may potentially exit the ECS through the Tsushima Strait without being utilized (Zhang et al., 2024). Where are the Kuroshio nutrients utilized by phytoplankton after entering the ECS and where do they regenerate? What are the distinct spatiotemporal features of the Kuroshio's new and regenerated nutrients? Further investigation of the actual roles of Kuroshio nutrients in the ECS ecosystem is desperately needed. Therefore, accurately tracing nutrients from various sources and distinguishing between new and regenerated nutrients are essential for assessing their roles.

An effective method is to establish models that can track the transport and cycling processes of nutrients from different sources (Kawamiya, 2001; Ménesguen et al., 2006). Consequently, a physical-biological coupled model with nutrient tracking model modules provides insights into studying marine ecosystems with multiple sources and mechanisms. The nutrient tracking model can individually track nutrients from different sources and express the physical transport and biochemical cycling processes of nutrients from different sources in a certain sea area. For instance, Zhang et al. (2019) used a nutrient tracking model to evaluate various nutrient sources (rivers, Kuroshio, Taiwan Strait, atmospheric deposition) in the ECS and found significant seasonal variations of DIN and DIP from different sources.

This study focuses on the impact of Kuroshio nutrients on the ECS ecosystem, using a physical-biological coupled module and the nutrient tracking module to separate Kuroshio nutrients into new nutrients (DIN_{KN}, DIP_{KN}) and regenerated nutrients (DIN_{KR}, DIP_{KR}). Kuroshio-originated new nutrients are defined as nutrients newly transported from the Kuroshio into the ECS, while Kuroshio-regenerated nutrients are defined as nutrients regenerated through phytoplankton respiration and detritus decomposition. This study analyzes the spatiotemporal variations of new nutrients and regenerated nutrients originating from the Kuroshio in the ECS, and the new and regenerated production, calculates the lateral fluxes of Kuroshio nutrients across the 200, 100, and 50-m isobaths, assesses the corresponding inventory, primary production, and the characteristics of DIN_{KN} and DIN_{KR} associated with water masses in the ECS. Finally, the quantitative contributions of the two Kuroshio nutrient sources to the ECS ecosystem were evaluated.

2. Materials and Methods

2.1. Physical-Biological Coupled Model

The research area is the continental shelf of the ECS (Figure 1). We divided this area into three distinct zones: the inner shelf shallower than the 50-m isobath, the middle shelf between 50 and 100-m isobaths, and the outer shelf between 100 and 200-m isobaths. The model comprises two components: a physical-biological coupled module and a nutrient tracking module. The physical module is based on the Princeton Ocean Model (Guo et al., 2003, 2006) and the biogeochemical module is based on Norwegian Ecological Model system (NORWECOM) (Skogen et al., 1995; Skogen & Søiland, 1998), which has been used in Zhao and Guo (2011) and Wang et al. (2019). The model has a horizontal resolution of 1/18° and is vertically divided into 21 layers. The biogeochemical module was coupled online with the physical model, meaning that the advection and diffusion of biological variables and their related biogeochemical processes were calculated synchronously at each model time step within a single simulation. The main computational equations and biological parameters used in the model can be found in the aforementioned articles.

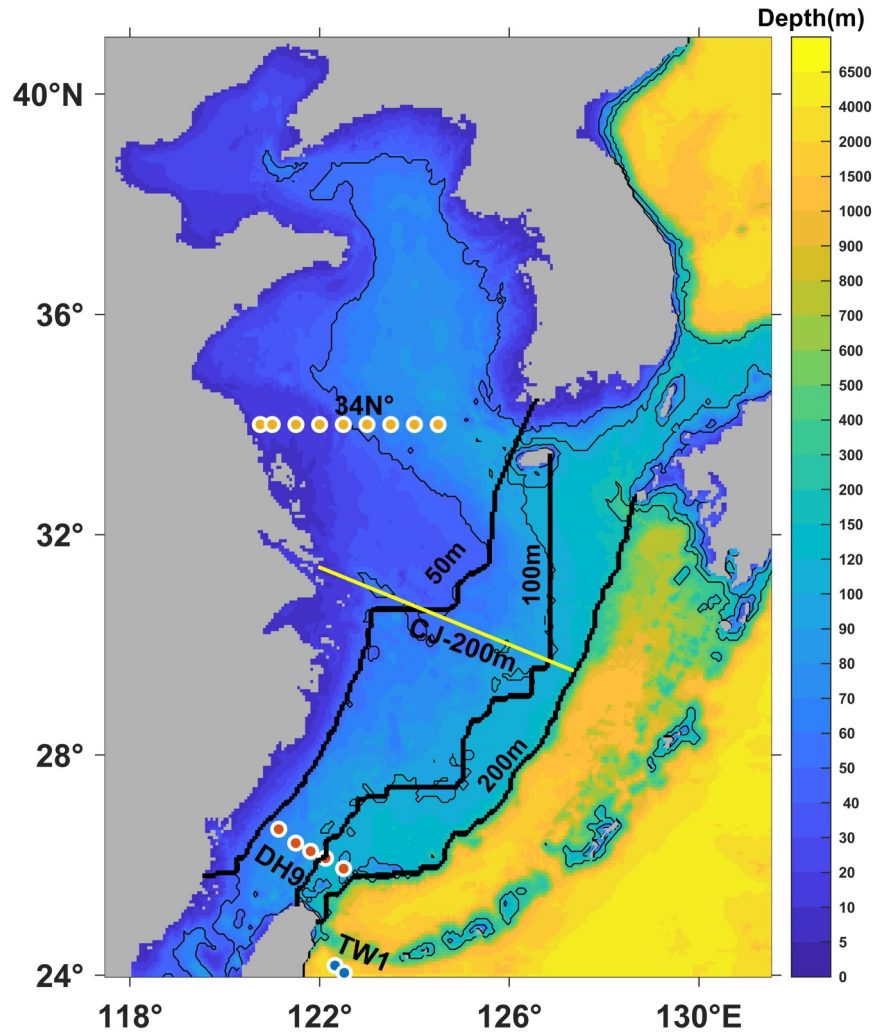

Figure 1. Map of the model domain and water depth (the analysis area is the region shallower than 200 m depth). The black contours represent 50, 100, and 200-m isobaths, respectively; blue dots indicate the TW1 observation stations, red dots indicate the DH9 observation stations, yellow dots represent the 34°N observation stations, and the yellow straight line represents the section from the Yangtze River to the 200-m isobath.

2.2. Nutrient Tracking Module

The nutrient tracking module is consistent with that used by Zhang et al. (2019, 2021, 2024), which independently calculates DIN and DIP in the ecosystem based on their different sources, taking into account both physical transport and biological cycling of nutrients. The biological variables in the tracking module include DIN, DIP, the diatom (DIA), the flagellate (FLA), and the detritus (DET), each marked according to its respective sources. Each source has a corresponding set of control equations for independently solving biological variables. This approach reflects the actual situations of different nutrient sources entering the ecosystem.

In the model, the DIN and DIP from the Kuroshio are denoted as DIN_K and DIP_K. The DIN_K and DIP_K newly entering the ECS from the south boundary are marked as new nutrients (DIN_{KN} and DIP_{KN}), which are utilized by phytoplankton once or not at all. After being utilized, the nutrients regenerated through phytoplankton respiration and detritus decomposition in the water column and sediments are termed as DIN_{KR} and DIP_{KR}. Nutrients entering from the eastern boundary, northern boundary, rivers, and the atmosphere are all classified under the boundary conditions for DIN_{others} and DIP_{others}, which are not discussed in this article.

In this study, the tracking module is applied separately to both DIN and DIP cases. The control equations for the ecological variables DIN, PHY (phytoplankton, representing FLA or DIA), and DET are as follows:

$$\frac{\partial \mathrm{DIN}_K}{\partial t} + \mathrm{adv}(\mathrm{DIN}_K) = \mathrm{diff}(\mathrm{DIN}_K) - \mathrm{PROD} + \mathrm{RESP} + \mathrm{DECO} \quad (1)$$

$$\frac{\partial \mathrm{DIN}_{\mathrm{KN}}}{\partial t} + \mathrm{adv}(\mathrm{DIN}_{\mathrm{KN}}) = \mathrm{diff}(\mathrm{DIN}_{\mathrm{KN}}) - \mathrm{PROD}_{\mathrm{KN}} \quad (2)$$

$$\frac{\partial \mathrm{DIN}_{KR}}{\partial t} + \mathrm{adv}(\mathrm{DIN}_{\mathrm{KR}}) = \mathrm{diff}(\mathrm{DIN}_{\mathrm{KR}}) - \mathrm{PROD}_{\mathrm{KR}} + \mathrm{RESP}_{\mathrm{KR}} + \mathrm{RESP}_{\mathrm{KN}} + \mathrm{DECO}_{\mathrm{KR}} + \mathrm{DECO}_{\mathrm{KN}} \quad (3)$$

$$\frac{\partial \mathrm{PHY}_K}{\partial t} + \mathrm{adv}(\mathrm{PHY}_K) = \mathrm{diff}(\mathrm{PHY}_K) + \mathrm{PROD} - \mathrm{RESP} - \mathrm{MORT} \quad (4)$$

$$\frac{\partial \mathrm{PHY}_{\mathrm{KN}}}{\partial t} + \mathrm{adv}(\mathrm{PHY}_{\mathrm{KN}}) = \mathrm{diff}(\mathrm{PHY}_{\mathrm{KN}}) + \mathrm{PROD}_{\mathrm{KN}} - \mathrm{RESP}_{\mathrm{KN}} - \mathrm{MORT}_{\mathrm{KN}} \quad (5)$$

$$\frac{\partial \mathrm{PHY}_{\mathrm{KR}}}{\partial t} + \mathrm{adv}(\mathrm{PHY}_{\mathrm{KR}}) = \mathrm{diff}(\mathrm{PHY}_{\mathrm{KR}}) + \mathrm{PROD}_{\mathrm{KR}} - \mathrm{RESP}_{\mathrm{KR}} - \mathrm{MORT}_{\mathrm{KR}} \quad (6)$$

$$\frac{\partial \mathrm{DET}_K}{\partial t} + \mathrm{adv}(\mathrm{DET}_K) = \mathrm{diff}(\mathrm{DET}_K) + \mathrm{MORT} - \mathrm{DECO} \quad (7)$$

$$\frac{\partial \mathrm{DET}_{\mathrm{KN}}}{\partial t} + \mathrm{adv}(\mathrm{DET}_{\mathrm{KN}}) = \mathrm{diff}(\mathrm{DET}_{\mathrm{KN}}) + \mathrm{MORT}_{\mathrm{KN}} - \mathrm{DECO}_{\mathrm{KN}} \quad (8)$$

$$\frac{\partial \mathrm{DET}_{\mathrm{KR}}}{\partial t} + \mathrm{adv}(\mathrm{DET}_{\mathrm{KR}}) = \mathrm{diff}(\mathrm{DET}_{\mathrm{KR}}) + \mathrm{MORT}_{\mathrm{KR}} - \mathrm{DECO}_{\mathrm{KR}} \quad (9)$$

In these equations, the left-hand side denotes the total change rate of concentration, while the right-hand side denotes the diffusive flux and biological sources/sinks. "adv" and "diff" represent advection and diffusion terms, PROD represents primary production by phytoplankton, RESP represents phytoplankton respiration, MORT represents phytoplankton mortality that turns phytoplankton into detritus, and DECO represents the decomposition of detritus that produces nutrients. The biological formulations are detailed in Text S1 of Supporting Information S1 and Skogen and Søiland (1998). Equations 1–3 are the calculation equations for $\mathrm{DIN_K}$, $\mathrm{DIN_{KN}}$, and $\mathrm{DIN_{KR}}$, respectively, in which the new nutrient is affected only by primary production and the regenerated nutrient is related to the other processes. The sum of equations for $\mathrm{DIN_{KN}}$ and $\mathrm{DIN_{KR}}$ becomes the equation for $\mathrm{DIN_K}$ by following $\mathrm{DIN_K} = \mathrm{DIN_{KN}} + \mathrm{DIN_{KR}}$. The DIP has a similar framework of equations with the DIN.

The initial conditions for the three variables ($\mathrm{DIN_K}$, $\mathrm{DIN_{KN}}$, and $\mathrm{DIN_{KR}}$) for the nutrients from the Kuroshio and their related phytoplankton and detritus are set to zero. The boundary conditions of nutrients, phytoplankton, and detritus from the Kuroshio east of Taiwan are derived from long-term observations averaged by the Japan Meteorological Agency. The open boundary conditions for $\mathrm{DIN_{KR}}$ are set to zero because nutrients regenerated within the shelf are its definition in this study. In other words, the nutrients supplied from the open boundary by the Kuroshio are treated as new nutrients ($\mathrm{DIN_{KN}}$). The model is run under climatological conditions to allow all the state variables to reach a steady state for subsequent result analysis. We have previously conducted some validations in Zhang et al. (2019, 2021, 2024). Here, we further conduct comparisons of model results with in situ observations and satellite data (Figures S1–S5 in Supporting Information S1), which indicate that the simulation results are generally consistent with the observational results.

3. Results

3.1. Spatial Distributions of $\mathrm{DIN_{KN}}$

The distributions of $\mathrm{DIN_{KN}}$ concentration in the surface, middle, and bottom layers of the ECS are shown in Figure 2, with May, August, November, and February representing spring, summer, autumn, and winter, respectively. The depth of the middle layer is defined as the smaller one of half the depth and 100 m depth. The depth of the bottom layer is defined as the smaller one of water depth and 200 m depth. The surface $\mathrm{DIN_{KN}}$ concentration peaks in winter and is mainly distributed in the southern parts of the middle shelf and the entire outer shelf region (Figure 2a). In spring and summer (Figures 2b and 2c), the thermocline hinders the upward transport of nutrients from the bottom layer. In addition, the phytoplankton consumes $\mathrm{DIN_{KN}}$, causing the surface

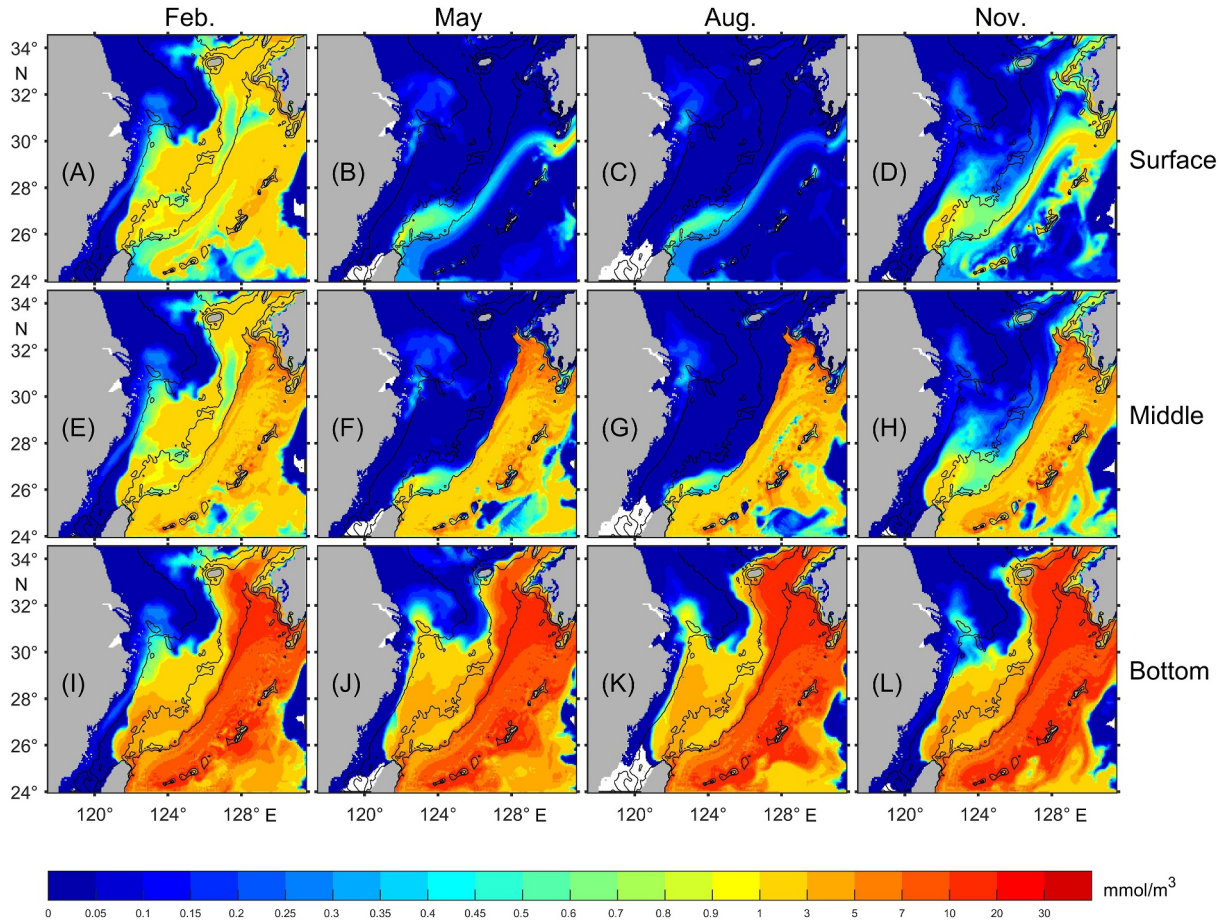

Figure 2. Horizontal distribution of DIN_{KN} concentrations in the surface, middle, and bottom layers in February, May, August, and November (unit: mmol/m^3).

DIN_{KN} to be almost depleted. Therefore, the concentration of DIN_{KN} in the surface layer is very low. Higher DIN_{KN} concentrations only exist in the area northeast of Taiwan due to the strong upwelling there (Liu et al., 2000). Slightly higher DIN_{KN} concentrations are also found near the estuary of the Yangtze River. In autumn, as water temperatures decrease and the thermocline gradually weakens, some bottom DIN_{KN} reach the surface, causing the surface DIN_{KN} concentration to rebound compared to spring and summer. The high-value area north of Taiwan Island becomes apparent in winter and autumn (Figure 2d).

The seasonal distribution of DIN_{NK} in the middle layer is similar to that in the surface layer in the area shallower than 200 m depth (Figures 2e–2h). In spring and summer, the DIN_{NK} concentration in the middle layer northeast of Taiwan is slightly higher than that at the surface. In areas deeper than 200 m depth, the DIN_{NK} concentration in the middle layer is high, but in areas shallower than 200 m depth, the concentration is low except in winter. This result indicates that the onshore transport of the Kuroshio-originated new nutrients across the 200-m isobath is difficult to reach the middle and surface layers. The bottom DIN_{KN} concentration remains high throughout the year (Figures 2i–2l), with large areas of high values in the middle and the outer shelves. Interestingly, the nutrient concentration in the outer shelf increases apparently in the area north of 30°N as compared to the area south of 30°N. High DIN_{KN} concentrations are also found outside the Yangtze River Estuary in spring and summer, indicating that the DIN_{KN} out of the Yangtze River Estuary is transported from the Kuroshio at the bottom layer. Yang et al. (2011, 2017) also confirmed that the Kuroshio Bottom Branch Current can carry high nutrient water along the bottom of the ECS shelf northward to the Yangtze River estuary and its adjacent waters. Our results reveal an interesting distribution of DIN_{KN} from the Yangtze River estuary to the Taiwan Strait in winter, suggesting that the southward current along the China coast from the Yangtze River estuary to the Taiwan Strait may carry nutrients from the Kuroshio. In summer, there is a high concentration of the DIN_{KN} branch in the bottom layer northeast of Taiwan (Figure 2k), which transports almost along the 100-m isobath. This is consistent

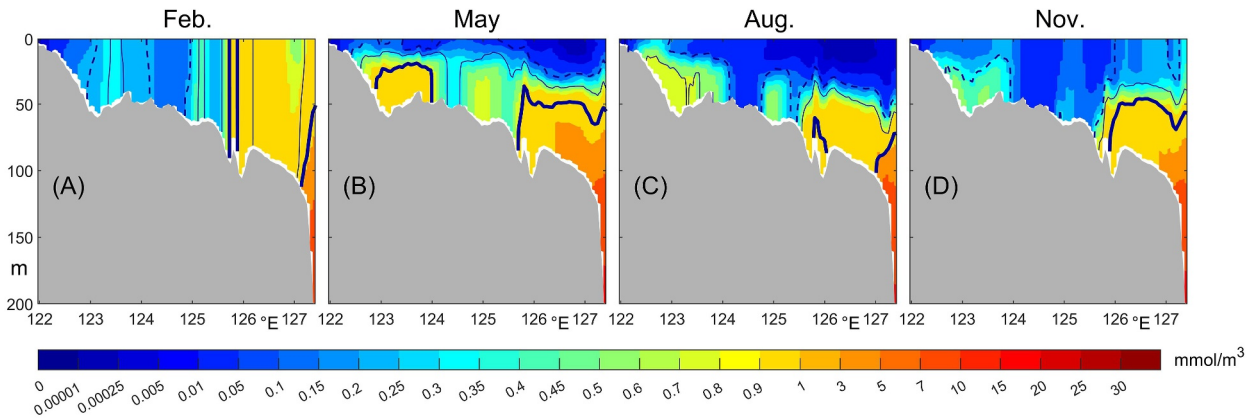

Figure 3. Vertical distributions of DIN_{KN} (a–d) in the section from the Yangtze River estuary to the 200-m isobath throughout the four seasons (unit: mmol/m^3). Note: Dashed lines, thin solid lines, and thick solid lines indicate the areas where DIN_{KN} accounts for 30%, 50%, and 70% of DIN_K.

with Yang et al. (2012), who reported the water from the Kuroshio east of Taiwan at 60–120 m. The high concentration of nutrients in the bottom layer is mainly due to the intrusion of the Kuroshio water, as well as the limited utilization of nutrients due to low light exposure in the bottom layer. It is noted that phytoplankton does not absorb the DIN_{KN} shown in Figure 2; once it does, the DIN_{KN} becomes DIN_{KR} through biological processes. The horizontal distribution of DIP_{KN}, described in Figure S6 of Supporting Information S1, exhibits a similarity to the horizontal distribution of DIN_{KN}.

The vertical distributions of DIN_{KN} across the section from the Yangtze River Estuary to the 200-m isobath are shown in Figure 3. In winter, due to the strong vertical mixing, the DIN_{KN} concentrations in the surface and bottom layers are homogeneous. High concentrations are found in the eastern part of the section, where DIN_{KN} can account for more than 50% of DIN_K, and then gradually decrease from east to west. Low DIN_{KN} concentrations were found near the Yangtze River Estuary and in the central section (Figure 3a). In spring, the DIN_{KN} concentration is low in the surface layer but high in the middle and bottom layers, showing a clear stratified structure. High DIN_{KN} concentration exists in the bottom layer of the western and eastern parts of the section, accounting for more than 70% of DIN_K. The DIN_{KN} concentration in the middle and bottom layers in the central region accounts for over 50% of DIN_K, indicating subsurface Kuroshio nutrient intrusion across the shelf (Figure 3b). There is also a clear stratified structure in summer, with a larger range of low-concentration areas on the surface. The DIN_{KN} concentration below the surface on both the east and west sides of the section still accounts for more than 50% of DIN_K, but the 70% proportion area has decreased compared to spring, due to the increase of regenerated nutrients in summer, which leads to a decrease in the proportion of DIN_{KN} (Figure 3c). In autumn, the stratification phenomenon gradually weakens, and the bottom layer concentration remains higher than the surface layer. The proportion on the east side of the section is still above 70%, while on the west side, the proportion of DIN_{KN} in the bottom layer decreases to only about 30%. The surface and bottom layers in the central area tended to have similar and low concentrations, gradually returning to the winter pattern (Figure 3d). The vertical distribution of DIP_{KN}, described in Figure S7 of Supporting Information S1, exhibits a similarity to the horizontal distribution of DIN_{KN}.

3.2. Spatial Distributions of DIN_{KR}

The concentration distribution of DIN_{KR} in the surface, middle, and bottom layers of the ECS is shown in Figure 4. The surface DIN_{KR} concentration peaks in winter, with higher concentrations across most of the ECS shelf. There are high-value areas west of Kyushu, north of 28°N in the outer shelf, and the coastal region (Figure 4a). The reason for the high DIN_{KR} concentration is the massive mortality of phytoplankton and the decomposition of detritus, leading to the regeneration of nutrients. In spring, DIN_{KR} exhibits a tongue-shaped area with higher concentrations in the Yangtze River Estuary. Surface phytoplankton utilizes DIN_{KR}, resulting in a significant reduction in concentration compared with winter (Figure 4b). In summer, higher DIN_{KR} concentrations are concentrated mainly in the southern Yellow Sea, but these concentrations are lower than those in spring (Figure 4c). In autumn, the DIN_{KR} concentration rises in the area northeast of the Yangtze River Estuary

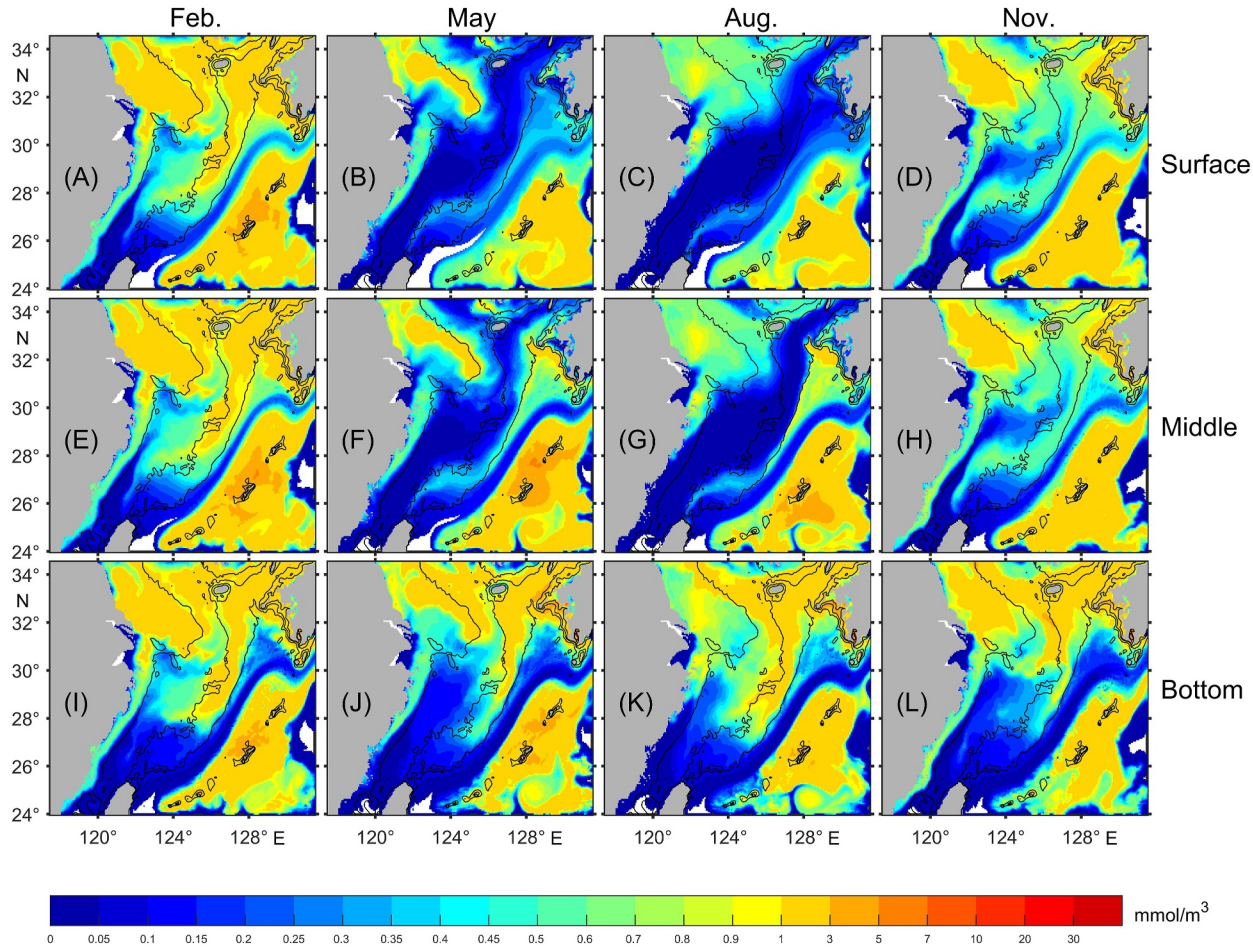

Figure 4. As in Figure 2 but for DIN_{KR}.

(Figure 4d). One reason is that the weakening of the thermocline enables the supply of DIN_{KN} from the bottom to the surface, and phytoplankton uses DIN_{KN} to produce regenerated nutrients through respiration. Another reason is the weakening of phytoplankton activity and gradual death, leading to the reduction in detritus decomposition and nutrient regeneration. The spatial distribution of DIN_{KR} in the middle layer is similar to that in the surface layer throughout the four seasons (Figures 4e–4h). Overall, the concentrations of DIN_{RK} in both the surface and middle layers are higher in autumn and winter than in spring and summer.

The DIN_{KR} concentrations in spring, summer, and autumn are significantly higher in the bottom layer than in the middle and surface layers. In winter, the DIN_{KR} concentrations in the surface and bottom layers are almost the same. There is an expansion of DIN_{KR} in the bottom layer northward through the southern Yellow Sea. The DIN_{KR} concentrations in the surface, middle, and bottom layers are very low in the area northeast of Taiwan throughout the four seasons. DIN_{KR} concentrations are significantly greater than DIN_{KN} in shelf areas north of 30°N. The horizontal distribution of DIP_{KR}, described in Figure S8 of Supporting Information S1, exhibits a similarity to the horizontal distribution of DIN_{KR}.

The vertical distributions of DIN_{KR} across the section from the Yangtze River Estuary to the 200-m isobath are shown in Figure 5. In winter, DIN_{KR} is mixed vertically with DIN_{KN}. In the eastern section, DIN_{KR} accounts for up to 50% of DIN_K (Figure 5a). In contrast to DIN_{KN}, DIN_{KR} predominates in regions in the central and western sections with variable levels of elevated DIN_{KR} concentrations. In the spring and summer, there was also a noticeable stratification phenomenon for DIN_{KR} (Figures 5b and 5c). The DIN_{KR} concentration in spring is lower than that in winter due to less detritus decomposition. The increase in DIN_{KR} concentration in summer compared to spring is attributed to the growth and respiration of phytoplankton, which regenerates DIN_{KR}. In spring and summer, DIN_{KR} is higher in the bottom layer than in the surface layer, especially on both the east and west sides of

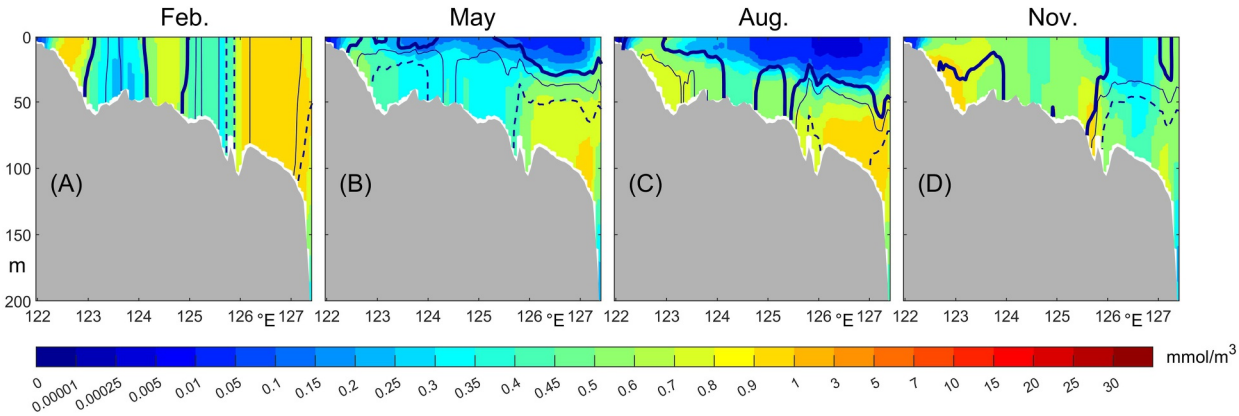

Figure 5. As in Figure 3 but for the DIN_{KR}.

the section. In autumn, the stratification phenomenon weakens, and the DIN_{KR} concentrations at the surface and bottom are close to each other. Higher concentrations are found in a small area of the bottom layer in the west and central sections, with some areas accounting for up to 70% of DIN_K (Figure 5d). The vertical distribution of DIP_{KR}, described in Figure S9 of Supporting Information S1, exhibits a similarity to the vertical distribution of DIN_{KR}.

3.3. Horizontal Distributions of PON_{KN}

After being initially utilized by phytoplankton, new nutrients are converted into particulate form, which is decomposed in water or seabed to regenerate nutrients. Particulate organic nitrogen (PON_{KN}) is a pathway for the conversion between DIN_{KN} and DIN_{KR}. It refers to phytoplankton and detritus converted from DIN_{KN} and is defined as the sum of DIA, FLA and DET in the model.

The distributions of PON_{KN} concentration in the surface, middle, and bottom layers of the ECS are shown in Figure 6. In winter, the surface PON_{KN} concentration is higher in most of the outer shelf regions (Figure 6a). In spring and summer, PON_{KN} concentration is relatively low across almost the entire shelf region (Figures 6b and 6c). In autumn, there were higher PON_{KN} concentrations in the middle shelf region northeast of Taiwan Island (Figure 6d). The seasonal variations in PON_{KN} in the middle layer are similar to those in the surface layer (Figures 6e–6h), with higher PON_{KN} concentrations in the outer shelf area in the northeast of Taiwan Island during spring and summer compared to the surface layer. Except for winter, the concentration of PON_{KN} was higher in the bottom layer than in the surface and middle layers (Figures 6j–6l). The concentration of PON_{KN} in spring and winter is similar, while in summer, the concentration of PON_{KN} in the eastern shelf area of the ECS is higher, reflecting a strong growth of phytoplankton. In autumn, there is a small high-value area in PON_{KN} in the southern area of Jeju Island (Figure 6l). The spatial distribution of PON_{KN} indicates that the new nutrients from the Kuroshio Current can cross the 50-m isobath and enter the inner shelf, providing nutrients for the phytoplankton growth in the northern part of the ECS and even the southern part of the Yellow Sea. The low concentration of PON_{KN} along the main axis of the Kuroshio is due to the absence of data along the open boundary. However, our primary focus is on the primary production over the shelf, and therefore, we do not consider the input of PON_{KN} from the open boundary.

The utilization of DIN_{KN} produces PON_{KN}, and the decomposition of PON_{KN} produces DIN_{KR}. Therefore, the regions with high PON_{KN} concentrations also have high DIN_{KR} concentrations. However, in some areas of the southern middle and outer shelves, although DIN_{KN} concentrations are high, PON_{KN} and DIN_{KR} concentrations are low, indicating that phytoplankton growth there is limited, and DIN_{KN} continues to be transported northward. In the inner shelf region, the distributions of bottom PON_{KN} concentrations indicate that PON_{KN} can extend to around 34°N in summer. In contrast, DIN_{KN} concentrations are lower in the inner shelf, while DIN_{KR} concentrations are higher, suggesting that DIN_{KN} is utilized to produce PON_{KN}, which is then decomposed into DIN_{KR}. The above results indicate that DIN_{KR} expands the influence area of Kuroshio nutrients and is an important source of nutrients for the ECS ecosystem, complementing the impact of Kuroshio nutrients on the middle and inner shelf

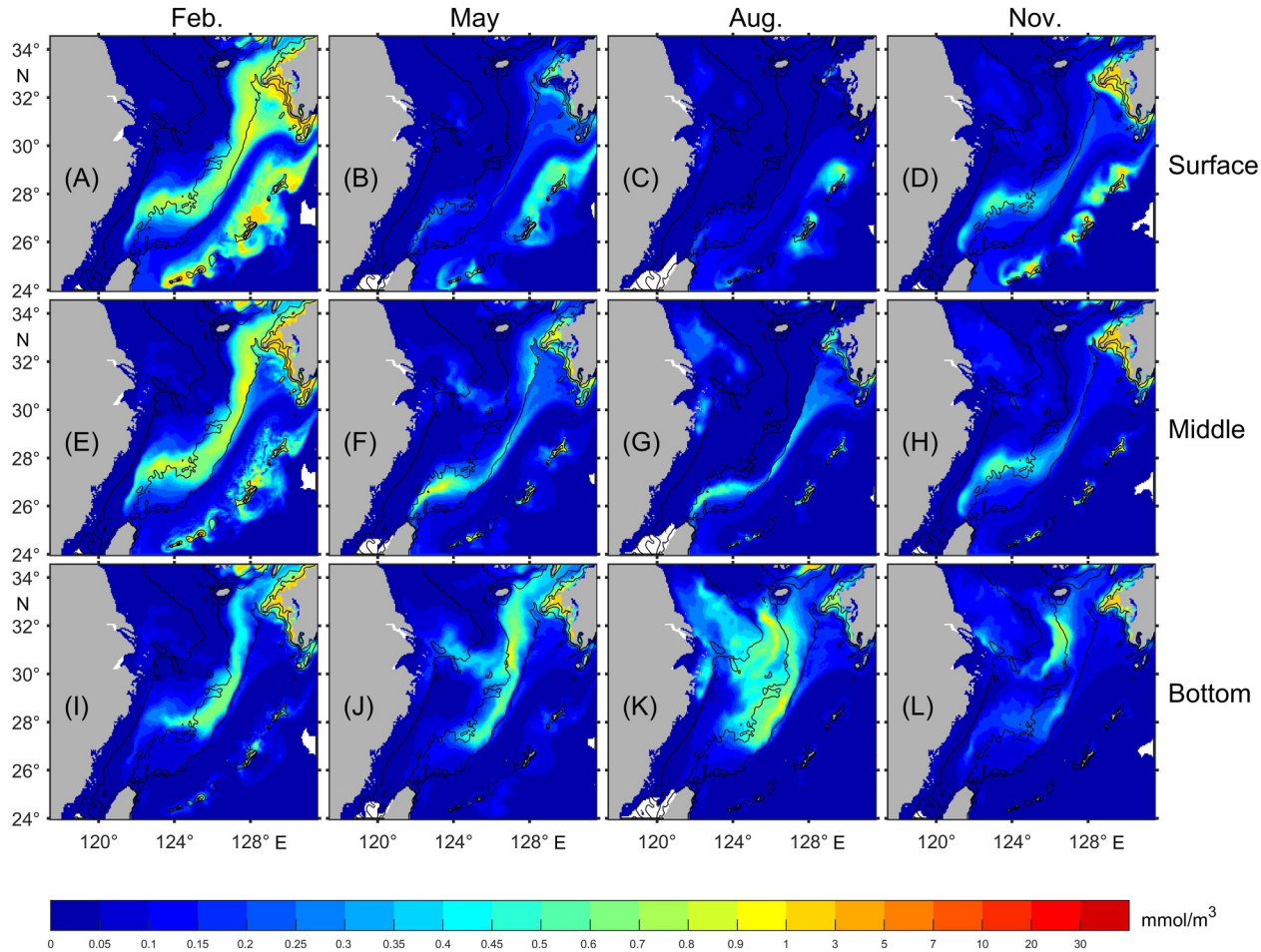

Figure 6. As in Figure 2 but for PON_{KN}.

ecosystems north of 30°N. The horizontal distribution of POP_{KN}, described in Figure S10 of Supporting Information S1, exhibits a similarity to the horizontal distribution of PON_{KN}.

3.4. Horizontal Distributions of New Production and Regenerated Production

The new production is defined as the phytoplankton growth using DIN_{KN} while the regenerated production is that using DIN_{KR}. The horizontal distributions of water-column integrated new production ($N\text{-}IPP_{KN}$) and regenerated production ($N\text{-}IPP_{KR}$) in the ECS are shown in Figure 7. In winter, $N\text{-}IPP_{KN}$ peaks and concentrates in the outer shelf region of the ECS (Figure 7a). Due to the high concentrations of DIN_K and temperature control, the levels of $N\text{-}IPP_{KN}$ and $N\text{-}IPP_{KR}$ in the outer shelf region were higher than those in the inner and middle shelf areas. Consequently, the $N\text{-}IPP_{KN}$ and $N\text{-}IPP_{KR}$ in most of the outer continental shelf area exceed 480 mg $C/m^2/d$ (Figures 7a and 7e). In spring, the levels of $N\text{-}IPP_{KN}$ decrease north of 28°N, with high $N\text{-}IPP_{KN}$ levels only appearing in the outer shelf off northern Taiwan Island. However, the levels of $N\text{-}IPP_{KN}$ near the middle shelf at 30°N were higher than those in winter (Figure 7b). In summer, $N\text{-}IPP_{KN}$ begins to extend along the onshore Kuroshio branch to the middle shelf and spreads to the 30°N region (Figure 7c). In autumn, the distribution range of higher $N\text{-}IPP_{KN}$ levels was the smallest, with these higher values only found in the area west of Kyushu and near the 100-m isobath in the southern part of the ECS (Figure 7d).

In winter, high $N\text{-}IPP_{KR}$ concentrations are concentrated in the outer shelf region of the ECS north of 28°N (Figure 7e). In spring, the area with high $N\text{-}IPP_{KR}$ expands, and forms a complementary relationship with the low concentration area of $N\text{-}IPP_{KN}$, spreading to the middle shelf in the northern ECS and the 50-m isobath region north of 31°N (Figure 7f). In summer, the value of $N\text{-}IPP_{KR}$ decreases in the western Kyushu region. However,

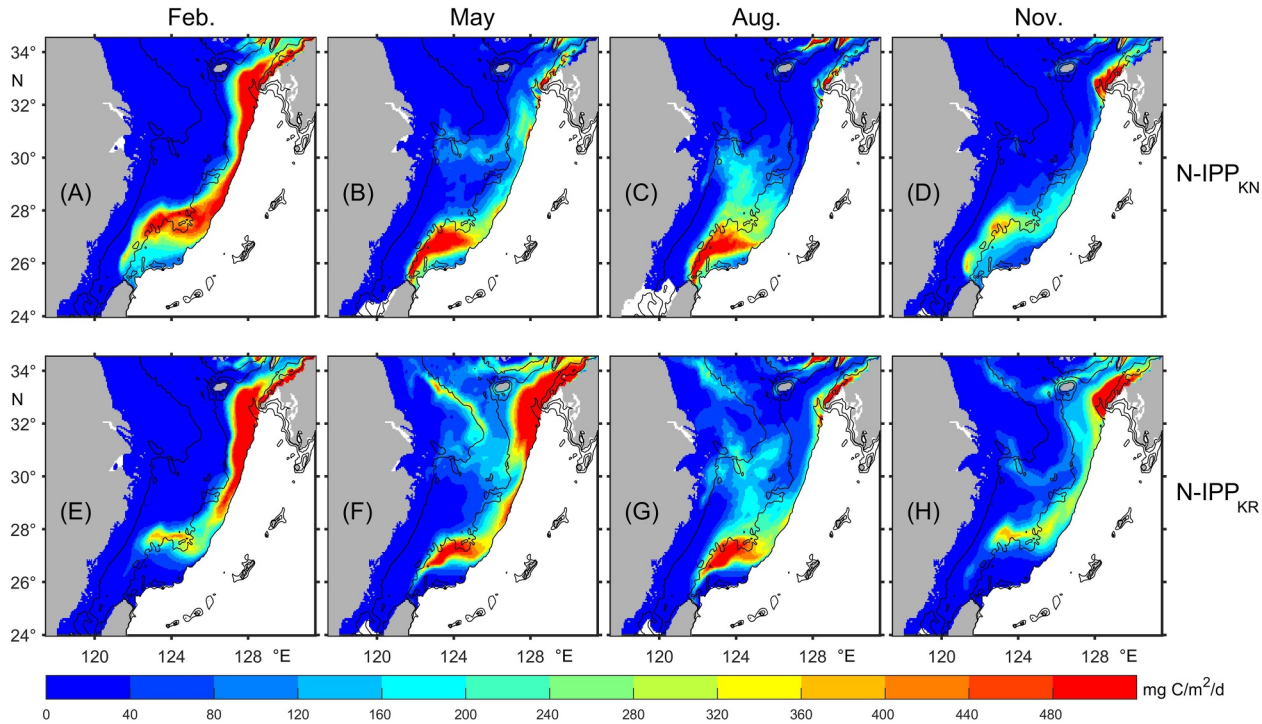

Figure 7. Distributions of water-column integrated primary production (mg C/m^2/d) supported by DIN_{KN} and DIN_{KR} in four seasons. Panels (a–d) N-IPP_{KN} represents the new production supported by DIN_{KN}, while (e–h) N-IPP_{KR} represents the regenerated production supported by DIN_{KR}.

due to the increase in sea temperature near the coast, the activity of phytoplankton is enhanced, causing the high-value area of N-IPP_{KR} to extend toward the coast. Consequently, higher N-IPP_{KR} values were found in parts of the middle shelf in the central ECS and the inner shelf in the northern ECS (Figure 7g). In autumn, with weaker phytoplankton activity, N-IPP_{KR} occurs in the outer shelf region (Figure 7h).

3.5. Monthly Variations in the Across-Isobath Fluxes of DIN_{KN} and DIN_{KR}

To quantify the intrusions of the Kuroshio-origin nutrient, the DIN_K, DIN_{KN} and DIN_{KR} fluxes across the 200, 100, and 50-m isobaths were calculated (Figure 8). Regardless of biological processes, the variations in the fluxes across the isobaths are mainly associated with physical processes. The annual average flux of DIN_K across the 200-m isobath is 12.93 kmol/s (Figure 8a), which is close to the Kuroshio DIN flux calculated by Zuo (2018) at

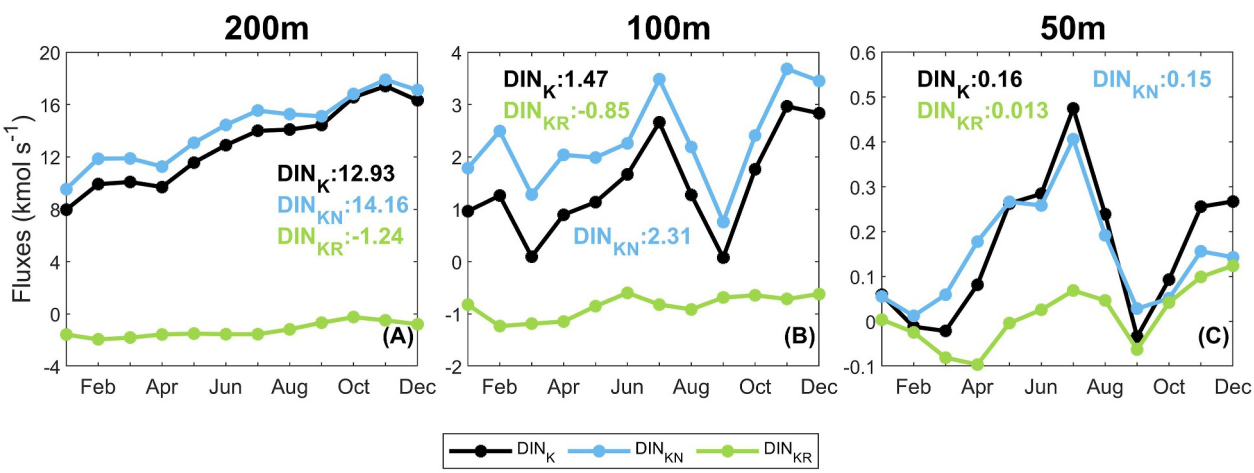

Figure 8. Monthly variations of fluxes of DIN_K, DIN_{KN} and DIN_{KR} across the (a) 200-m, (b) 100-m, and (c) 50-m isobaths (unit: kmol/s).

14.22 kmol/s. The DIN_{KN} flux was approximately 14.16 kmol/s. The monthly variations in DIN_K and DIN_{KN} fluxes are similar, with a maximum in November. The annual average flux of DIN_{KR} is −1.24 kmol/s with a weak flux in autumn. The concentration of DIN_{KR} is larger in the shelf than in the area deeper than 200 m. Therefore, the DIN_{KR} flux across the 200-m isobath is negative. The DIN_{KR} flux accounts for only 9.6% of the DIN_K flux. The DIN_{KN} flux is an order of magnitude larger than the DIN_{KR} flux.

The annual DIN_K flux across the 100-m isobath is 1.47 kmol/s (Figure 8b), with a peak value of approximately 3.00 kmol/s in July and November. After July, the DIN_K flux decreases gradually and reaches zero in September before gradually increasing again. The DIN_K flux is positive throughout the year. The annual average DIN_{KN} flux across the 100-m isobath is 2.31 kmol/s, with monthly variations similar to DIN_K. In September, its flux can still reach about 1.00 kmol/s. Within DIN_{KN} onshore flux across the 200-m isobath, 16.3% of DIN_{KN} is transported to the middle shelf area, as the main part of DIN transport from the Kuroshio to the shore across the 100-m isobath. The DIN_{KR} flux across the 100-m isobath is negative throughout the year (−0.85 kmol/s), indicating that DIN_{KR} is transported from shallower areas (shallower than 100 m) to deeper areas.

The annual DIN_K flux across the 50-m isobath is 0.16 kmol/s (Figure 8c). It is negative in February, March, and September and is highest in July. The annual DIN_{KN} flux is 0.15 kmol/s, with monthly variations similar to DIN_K but remaining positive throughout the year. There is still 1.1% of DIN_{KN} that can cross the 50-m isobath and transport to the inner shelf area from the 200-m isobath. The average DIN_{KR} flux is 0.013 kmol/s, indicating an onshore direction into the inner shelf. The DIN_{KR} flux across the 50-m isobath accounts for 8.1% of the DIN_K flux. Monthly variations of fluxes of DIP_K, DIP_{KN} and DIP_{KR} across the 200, 100, and 50-m isobaths are shown in Figure S11 of Supporting Information S1. The monthly variations in DIP flux are broadly similar to those of DIN. However, the flux of DIP_{KR} at the 50-m isobath differs slightly from DIN_{KR}, with a negative annual mean.

4. Discussion

4.1. The Water Masses Characteristics of DIN_{KN} and DIN_{KR} Dominant Regions

To further clarify the different roles of DIN_{KN} and DIN_{KR} in the ECS, the water mass characteristics of their dominated regions were analyzed through the temperature-salinity diagram. The dominated region of DIN_{KN} or DIN_{KR} in the shelf is defined as where the concentration is higher than half of DIN_K. In winter, high concentrations of DIN_{KN} are primarily found in the Kuroshio Surface Water (salinity > 34), which lies at the relatively heavy isopycnals. A portion of this Kuroshio Surface Water flows toward the broad shelf region, carrying low concentrations of DIN_{KN} and high concentrations of DIN_{KR} (Figures 9a and 9e). As indicated by the alignment of points with lighter isopycnals, this water mass mixes with low-salinity water to form shelf mixed water (Umezawa et al., 2014). Kuroshio waters can even reach the inner shelf areas covered by coastal water in winter. In spring and summer, low concentrations of DIN_{KN} are concentrated in the Kuroshio Surface Water (Figures 9b and 9c), and the concentration of DIN_{KR} carried by the Kuroshio is also low (Figures 9f and 9g), which is related to the thermocline hindering of upward nutrient transport from the subsurface of the Kuroshio and the growth of phytoplankton. In autumn, the temperature of Kuroshio waters decreases, and the concentrations of both DIN_{KN} and DIN_{KR} are higher than those in spring and summer but slightly lower than those in winter (Figures 9d and 9h). The shift of points toward lower-temperature isopycnals reflects seasonal cooling.

The concentrations of DIN_{KN} associated with bottom Kuroshio Subsurface Water are high throughout the year, consistently clustered along the high-salinity, high-density isopycnals. As the temperature of the dominant water masses expands in spring and summer, it further indicates that they can reach further onshore (Figures 9j and 9k). However, most of the high-concentration DIN_{KN} associated with Kuroshio waters remains concentrated in the Kuroshio Subsurface Water masses (salinity > 34.4). The high concentrations of DIN_{KN} also indicate that some of the high-salinity, high-concentration Kuroshio nutrients previously observed in the Kuroshio region may not be utilized by phytoplankton and are therefore ineffective for the entire ECS ecosystem. In winter, due to strong vertical mixing, the temperature, salinity, and associated DIN_{KR} are similar to those in the surface layer (Figure 9m). In spring and summer, both Kuroshio Subsurface Water and shelf mixed water carry a large amount of dominant DIN_{KR} (Figures 9n and 9o). In autumn, the concentration of DIN_{KR} in the bottom layer is slightly higher than that in the surface layer, which is reflected in the denser isopycnals occupied by the bottom water (Figure 9p). In general, DIN_{KR} mainly dominates in shelf mixed water and coastal water systems, while DIN_{KN} associated with Kuroshio waters is concentrated in Kuroshio Surface Water and Kuroshio Subsurface Water.

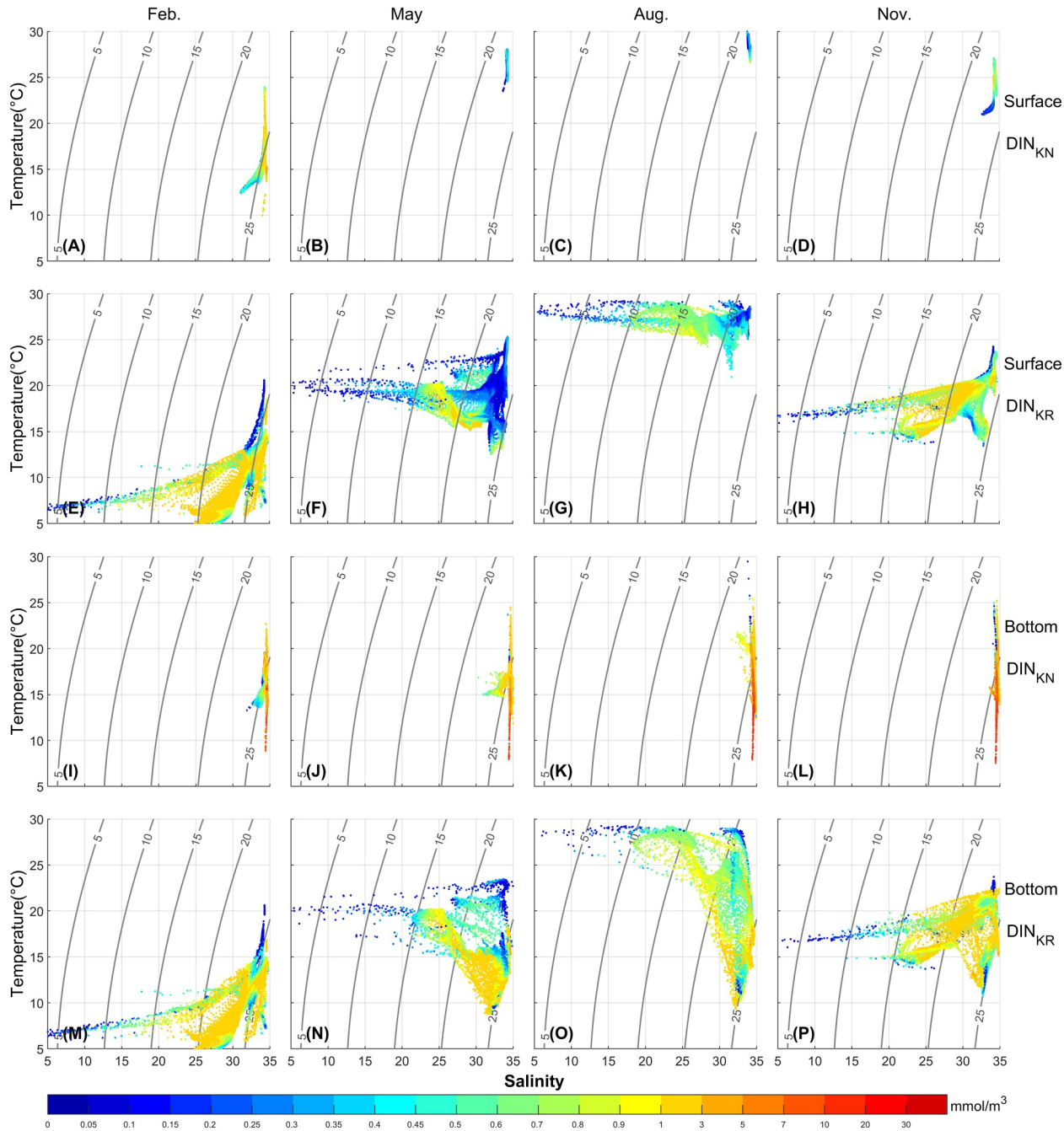

Figure 9. Distribution of dominant DIN_{KN} and DIN_{KR} (mmol/m^3) in a T–S diagram. Colors represent the DIN concentration. The dominated region of DIN_{KN} or DIN_{KR} is defined as where its concentration is higher than half of DIN_K. Isopycnals are denoted by the background contour lines.

4.2. Comparison Between the Primary Production Supported by DIN_{KN} and DIN_{KR}

The nutrient inventory over the ECS is the accumulation of input flux and is influenced by physical and biological processes (Figure 10a). The inventory of DIN_K is highest in December but lowest in April, with an annual mean of 11.3×10^7 kmol (Table 1). The inventory of DIN_{KN} shares a similar variation with that of DIN_K, but their variations are opposite to that of PON_{KN}. In April, the inventory of DIN_{KN} is lowest while PON_{KN} is highest, indicating the conversion from DIN_{KN} to PON_{KN} through photosynthesis. Both DIN_{KR} inventory and its proportion in DIN_K inventory exhibited parallel seasonal variations, characterized by high values in February–March

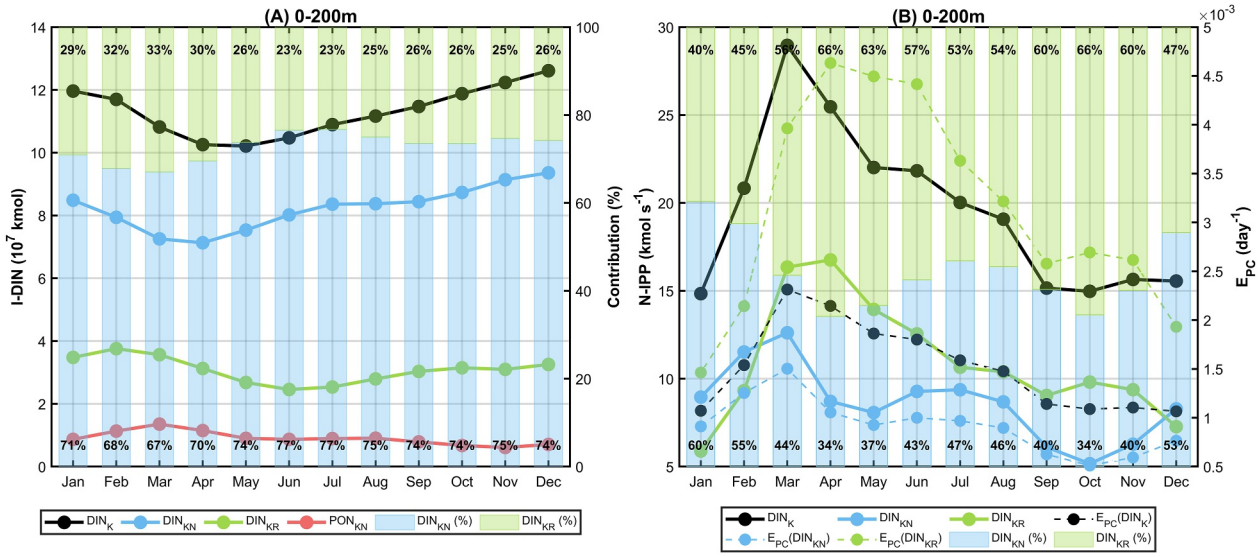

Figure 10. Monthly variations of the (a) inventory of DIN_K (I-DIN_K, 10^7 kmol), (b) the primary production integrated over the water column (N-IPP_K, kmol/s) and production efficiency (E_{PC}) supported by DIN_K, DIN_{KN} and DIN_{KR} in the entire shelf area (0–200 m). The lines with black, blue, green, and red circles in (a) represent the DIN_K, DIN_{KN}, DIN_{KR}, and PON_{KN}. Panel (b) distinguishes N-IPP (solid lines) from E_{PC} (dashed lines). The colors black, blue, and green correspond to DIN_K, DIN_{KN}, and DIN_{KR}, respectively. Stacked bars show the proportions of DIN_{KN} (blue) and DIN_{KR} (green) to DIN_K in inventory (a) and primary production (b), respectively.

and low values in summer. The decrease in DIN_{KR} inventory in spring is related to phytoplankton growth and decreased detritus decomposition.

The N-IPP_{KN} supported by DIN_{KN} (blue line) and N-IPP_{KR} supported by DIN_{KR} (green line) are shown in Figure 10b. Primary production (N-IPP_K) using DIN_K (black line) reaches its peak in March and then begins to decline, with an annual mean of 19.52 kmol/s (Table 1). DIN_{KR} supports a higher N-IPP_{KR} than DIN_{KN} from March to November, whereas N-IPP_{KR} is less than N-IPP_{KN} in other months. In October, N-IPP_{KN} begins to rise as weakening of stratification allows DIN_{KN} to be transported to the surface to support N-IPP_{KN}. After that, N-IPP_{KN} peaks in March. The peak of N-IPP_{KR} lags behind N-IPP_{KN} by 1 month, reaching its maximum in April. This lag may be due to the influence of temperature, as the waters closer to the open ocean are warmer, causing the peak in primary production to arrive earlier. N-IPP_{KR} has two peaks in April and October, with its contribution to N-IPP_K reaching 66.0% during these months. Although the annual averaged inventory of DIN_{KR} is smaller than that of DIN_{KN}, it supports 56.0% of the N-IPP_K.

Production efficiency (E_{PC}) is defined as the ratio of primary production to the inventory of nutrients. It reflects the cycling rate corresponding to a specific nutrient source. In the ECS shelf, the E_{PC} of DIN_{KR} is almost three times higher than that of DIN_{KN}, indicating that large amounts of DIN_{KN} are not utilized efficiently, while DIN_{KR} is utilized multiple times. The monthly variation in E_{PC} for DIN_{KN} and DIN_{KR} mirrored that of their corresponding N-IPP, respectively. The primary production integrated over the water column (P-IPP_K) and inventory of DIP (I-DIP_K) are shown in Figure S12 and Table S1 of Supporting Information S1.

Table 1
Inventory of DIN_K (I-DIN_K), Primary Production (N-IPP_K) and Production Efficiency (E_{PC}) of DIN_{KN}, DIN_{KR} and DIN_K

	DIN_{KN}	DIN_{KR}	DIN_K
I-DIN_K (10^7 kmol)	8.23 (72.8%)	3.07 (27.2%)	11.30
N-IPP_K (kmol/s)	8.58 (44.0%)	10.94 (56.0%)	19.52
E_{PC} (day^{-1})	1/111	1/32	1/67

Note. The numbers in parentheses are the corresponding percentages.

4.3. Does the New Production Balance the Export Production Over the ECS?

New and export production are usually balanced in the open ocean to maintain a steady state, but not necessarily in the shelf region due to the complex dynamics and shallow nature. For example, in the ice zone of the Western Antarctic Peninsula, the temporal variation in physical upwelling rates and spatial decoupling can lead to a disparity between new production and export production (Ducklow et al., 2018; Stukel et al., 2016). In the northern Arabian Sea, the accumulation of biomass in the surface ocean may lead to a lag between the rates of new production and export production (Sambrotto, 2001). In

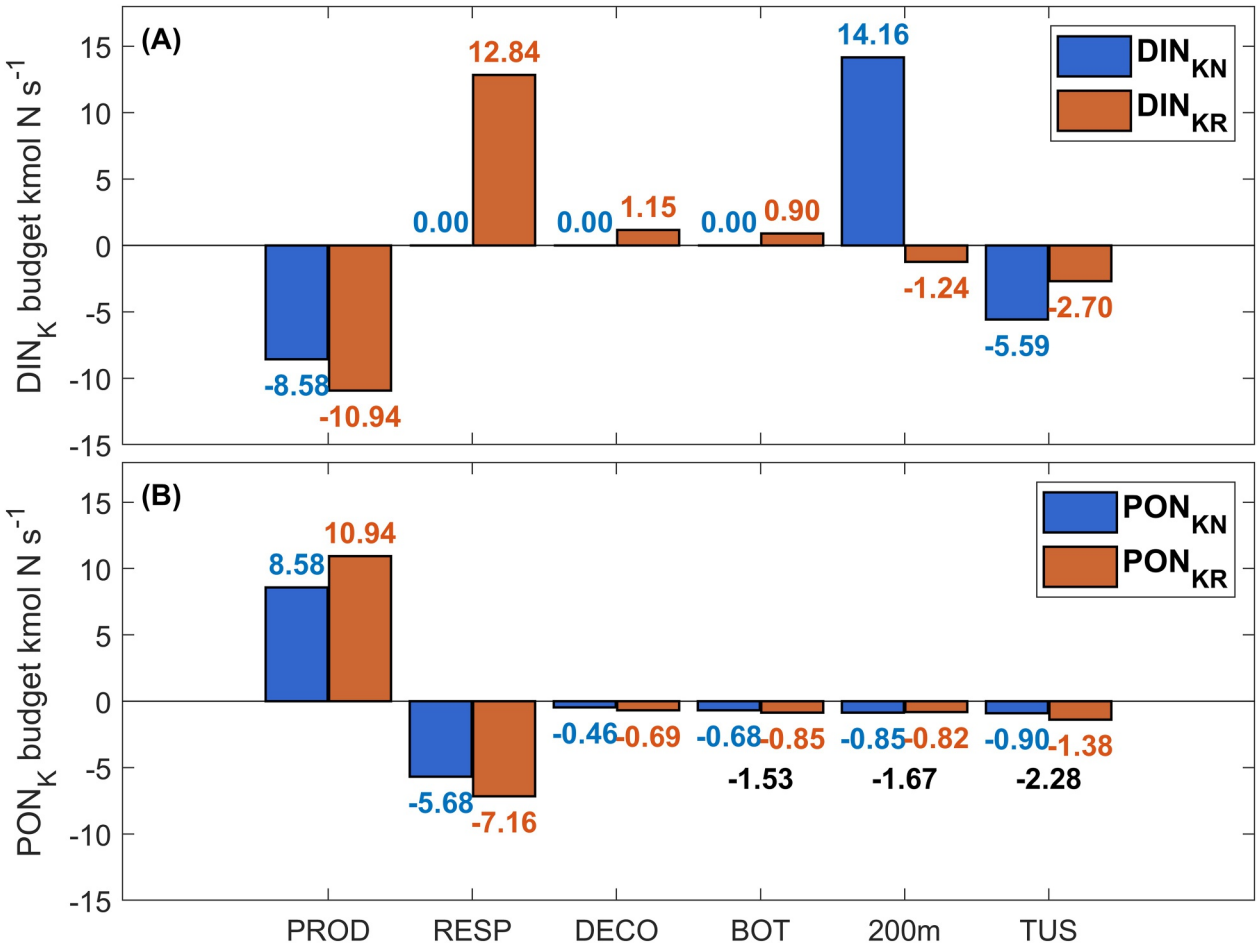

Figure 11. Nitrogen budgets for (a) DIN_K and (b) PON_K in the ECS. Budget components include biological processes (primary production (PROD), respiration (RESP), decomposition (DECO)) and physical fluxes (sediment-water interface exchange (BOT); cross-200 m isobath transport (200 m); and Tsushima Strait throughflow (TUS)). Blue bars and numbers denote the budget terms for DIN_{KN} and PON_{KN}, while orange bars and numbers represent those for DIN_{KR} and PON_{KR}. Black numbers in (b) represent physical terms of PON_K representing their aggregate total (unit: kmol N s^{-1}).

the California Current system, the spatial pattern reveals imbalances concerning new production and export production, and vertical advective fluxes of total organic nitrogen can alter the local balance of new production and vertical export production (Frischknecht et al., 2018). Therefore, the balance between new and export production may be disrupted by various factors, such as physical processes, biomass accumulation and spatial patterns.

Chen (2003) suggested that the remineralized nutrients on the ECS shelf reenter the euphotic zone, quickly causing the discrepancy between the new and export production in the ECS when using the definition of new production by Dugdale and Goering (1967). Here we define the Kuroshio's new nutrients of the ECS as the nutrients newly coming from the Kuroshio out of the shelf. The primary production supported by new nutrients is called new production, while the export of organic matter produced by photosynthesis is called export production (Eppley & Peterson, 1979).

Here, we present the nitrogen budgets for DIN_K and PON_K, partitioned into new and regenerated components (Figure 11). The budget terms consist of biological and physical processes. Biological fluxes such as primary production and respiration dominate the budgets. Physical fluxes mainly include lateral transport across the open boundaries and sediment-water exchange. To simplify the analysis, other lateral fluxes of DIN_K and PON_K out of the ECS (e.g., northward transport across 34°N and southward transport through the Taiwan Strait) were excluded, as their values are at least an order of magnitude smaller than the dominant terms.

For DIN_{KN} (Figure 11a), the major source is inflow across the 200-m isobath. Biologically, it is solely consumed by primary production and is not affected by respiration and decomposition. Following this definition, all regenerated nitrogen is accounted for in the DIN_{KR} pool. The primary sink for DIN_{KN} is outflow through the Tsushima Strait (TUS). DIN_{KR} originates from biological regeneration processes. It is primarily consumed by primary production, with a smaller fraction exported out of the East China Sea via the Tsushima Strait and across the 200 m isobath. The source and sink patterns for PON_{KN} and PON_{KR} are similar (Figure 11b). Biological processes act as sources, while physical processes (transport and sedimentation) serve as the main sinks.

The export production over the ECS shelf supported by DIN_K was 4.58 kmol/s. It is calculated as the net removal of the PON_K fluxes through sediment (1.53–0.90 = 0.63 kmol/s) and lateral boundaries (200-m isobath 1.67 kmol/s and the Tsushima Strait 2.28 kmol/s), including both PON_{KN} and PON_{KR}. The slight difference between this value and our previously calculated value of 4.40 kmol/s (Zhang et al., 2024) may result from the source-tracking module employed here, which computes Kuroshio DIN by dividing it into two parts and leads to certain nonlinear calculations. The new production supported by Kuroshio is 8.58 kmol/s, which is essentially the total production of PON_{KN}, which is approximately twice as much as the export production. They are not balanced either. So, what are the items that are supposed to balance the new production? In other words, where does the produced PON_{KN} go?

It is usually assumed that the PON_{KN} produced over the ECS shelf area is equal to that left across the ECS shelf on a yearly scale. However, PON_{KN} may convert to DIN_{KR} on the shelf and further convert to PON_{KR} through biological processes. Thus, the produced PON_{KN} can leave the ECS in three forms: PON_{KN} itself, PON_{KR} and DIN_{KR}. In the calculation of export production over the ECS, only the particulate form of nitrogen, that is, the sum of PON_{KN} and PON_{KR}, is taken into consideration and the dissolved one is ignored. Thus, ignoring the offshore transport of DIN_{KR} likely leads to a mismatch between the new and export production estimated from PON_K.

DIN_{KR} is carried out of the ECS shelf by lateral transport, giving a value of 3.94 kmol/s (the fluxes across the 200-m isobath 1.24 kmol/s and the Tsushima Strait 2.70 kmol/s). By including this part, the new production (8.58 kmol/s) can be balanced by the export production (4.58 kmol/s) and the lateral transport of regenerated nutrients (3.94 kmol/s). In the open ocean, there is no such lateral transport of nutrients, and the new production is balanced by the export production. However, in the ECS shelf, the new production should be balanced by the sum of export production and the lateral transport of the regenerated nutrients. This is a noteworthy reason for the imbalance between new and exported production over shelf seas estimated from the particulate form of material.

A limitation of our model lies in its simplified representation of the nitrogen cycle. The omission of the dissolved organic nitrogen (DON) pool and explicit microbial remineralization may affect the precise partitioning of nitrogen fluxes in the realistic ocean. Nevertheless, our explanation of the nitrogen budget in this study is not directly affected by the omission of DON because the lateral transport of the regenerated nutrient occurs in the realistic ocean.

5. Conclusions

Based on the physical-biological coupled model and nutrient tracking module, the spatiotemporal distribution characteristics of Kuroshio-origin new and regenerated nutrients and new and regenerated production in the ECS shelf were analyzed. New and regenerated nutrients undergo transformation through biological processes. These transformations occur in the high-concentration area of particulate organic matter supported by new nutrients. The characteristics of water masses in the regions dominated by DIN_{KN} and DIN_{KR} were analyzed through temperature-salinity diagrams. DIN_{KR} mainly dominates in shelf mixed water and coastal water, while DIN_{KN} is concentrated in Kuroshio Surface Water and Kuroshio Subsurface Water.

Monthly variations of nutrient fluxes across 200, 100, and 50-m isobaths were quantified, together with the nutrient inventory and primary production. The fluxes of Kuroshio-origin new nutrients across the 200, 100, and 50-m isobaths are an order of magnitude larger than those of Kuroshio-origin regenerated nutrients and are positive throughout the year. The fluxes of Kuroshio-origin regenerated nutrients at the 200 and 100-m isobaths are negative throughout the year. In the ECS shelf, the Kuroshio-origin new nutrients account for 72.8% of the inventory of Kuroshio-origin DIN and support 44.0% of primary production related to Kuroshio-origin DIN. On the other hand, Kuroshio-origin regenerated nutrients account for 27.2% of the total inventory of Kuroshio-origin DIN and support 56.0% of the primary production related to Kuroshio-origin DIN. The new and export production

supported by Kuroshio nutrients are not balanced in the ECS shelf. Their difference can be explained by the lateral transport of the regenerated nutrients, which can be considered as a new cause for the mismatch of new and export production in the shelf seas.

Conflict of Interest

The authors declare no conflicts of interest relevant to this study.

Availability Statement

Processed model results are available at https://zenodo.org/doi/10.5281/zenodo.18523756.

Acknowledgments
This work was supported by the National Key Research and Development Program of China (2023YFC3108203), the National Natural Science Foundation of China (Grant 42006018, 42276009, and 42176198), the Key Laboratory of Ocean Observation and Information of Hainan Province (Open Fund Project number HKLOOI-OF-2023-03), the Project of Tianjin Municipal Bureau of Planning and Natural Resources (KJ[2023]35). X. Guo is supported by Grant-in-Aid for Scientific Research (MEXT KAKENHI Grant 22H05206). JZ thanks the support of the Ministry of Education, Culture, Sports, Science and Technology, Japan (MEXT) under a Joint Usage/Research Center, Leading Academia in Marine and Environment Pollution Research (LaMer) Project.

References

Chen, C. T. A. (2003). New vs. export production on the continental shelf. *Deep Sea Research Part II: Topical Studies in Oceanography*, *50*(6–7), 1327–1333. https://doi.org/10.1016/S0967-0645(03)00026-2

Ducklow, H. W., Stukel, M. R., Eveleth, R., Doney, S. C., Jickells, T., Schofield, O., et al. (2018). Spring–summer net community production, new production, particle export and related water column biogeochemical processes in the marginal sea ice zone of the Western Antarctic Peninsula 2012–2014. *Philosophical Transactions of the Royal Society A: Mathematical, Physical and Engineering Sciences*, *376*(2122), 20170177. https://doi.org/10.1098/rsta.2017.0177

Dugdale, R. C., & Goering, J. J. (1967). Uptake of new and regenerated forms of nitrogen in primary productivity. *Limnology and Oceanography*, *12*(2), 196–206. https://doi.org/10.4319/lo.1967.12.2.0196

Eppley, R. W., & Peterson, B. J. (1979). Particulate organic matter flux and planktonic new production in the deep ocean. *Nature*, *282*(5740), 677–680. https://doi.org/10.1038/282677a0

Frischknecht, M., Münnich, M., & Gruber, N. (2018). Origin, transformation, and fate: The three-dimensional biological pump in the California current system. *Journal of Geophysical Research: Oceans*, *123*(11), 7939–7962. https://doi.org/10.1029/2018JC013934

Gong, G. C., Wen, Y. H., Wang, B. W., & Liu, G. J. (2003). Seasonal variation of chlorophyll a concentration, primary production and environmental conditions in the subtropical East China Sea. *Deep Sea Research Part II: Topical Studies in Oceanography*, *50*(6–7), 1219–1236. https://doi.org/10.1016/S0967-0645(03)00019-5

Guo, X., Hukuda, H., Miyazawa, Y., & Yamagata, T. (2003). A triply nested ocean model for simulating the Kuroshio-Roles of horizontal resolution on JEBAR. *Journal of Physical Oceanography*, *33*(1), 146–169. https://doi.org/10.1175/1520-0485(2003)033<0146:ATNOMF>2.0.CO;2

Guo, X., Miyazawa, Y., & Yamagata, T. (2006). The Kuroshio onshore intrusion along the shelf break of the East China Sea: The origin of the Tsushima warm current. *Journal of Physical Oceanography*, *36*(12), 2205–2231. https://doi.org/10.1175/JPO2976.1

Guo, X., Zhu, X. H., Wu, Q. S., & Huang, D. (2012). The Kuroshio nutrient stream and its temporal variation in the East China Sea. *Journal of Geophysical Research*, *117*(C1). https://doi.org/10.1029/2011JC007292

Kawamiya, M. (2001). Mechanism of offshore nutrient supply in the western Arabian Sea. *Journal of Marine Research*, *59*(5), 675–696. https://doi.org/10.1357/002224001762674890

Lee, J. S., & Takeshi, M. (2007). Intrusion of Kuroshio water onto the continental shelf of the East China Sea. *Journal of Oceanography*, *63*(2), 309–325. https://doi.org/10.1007/s10872-007-0030-9

Liu, K. K., Tang, T. Y., Gong, G. C., Chen, L. Y., & Shiah, F. K. (2000). Cross-shelf and along-shelf nutrient fluxes derived from flow fields and chemical hydrography observed in the southern East China Sea off northern Taiwan. *Continental Shelf Research*, *20*(4–5), 493–523. https://doi.org/10.1016/S0278-4343(99)00083-7

Ménesguen, A., Cugier, P., & Leblond, I. (2006). A new numerical technique for tracking chemical species in a multi-source, coastal ecosystem, applied to nitrogen causing Ulva blooms in the Bay of Brest (France). *Limnology and Oceanography*, *51*(1part2), 591–601. https://doi.org/10.4319/lo.2006.51.1_part_2.0591

Sambrotto, R. N. (2001). Nitrogen production in the northern Arabian Sea during the Spring Intermonsoon and southwest monsoon seasons. *Deep Sea Research Part II: Topical Studies in Oceanography*, *48*(6–7), 1173–1198. https://doi.org/10.1016/S0967-0645(00)00135-1

Simpson, J. H., & Sharples, J. (2012). *Introduction to the physical and biological oceanography of shelf seas*. Cambridge University Press. https://doi.org/10.1017/CBO9781139034098

Skogen, M. D., & Søiland, H. (1998). A user's guide to NORWECOM v2.0, a coupled 3 dimensional physical chemical biological ocean-model. Technical Report Fiskenog Havet 18/98. In *The NORWegian ecological model system*. Institute of Marine Research, Bergen. (p. 42).

Skogen, M. D., Svendsen, E., Berntsen, J., Aksnes, D., & Ulvestad, K. B. (1995). Modelling the primary production in the North Sea using a coupled three-dimensional physical-chemical-biological ocean model. *Estuarine, Coastal and Shelf Science*, *41*(5), 545–565. https://doi.org/10.1016/0272-7714(95)90026-8

Stukel, M. R., Benitez-Nelson, C. R., Décima, M., Taylor, A. G., Buchwald, C., & Landry, M. R. (2016). The biological pump in the Costa Rica dome: An open-ocean upwelling system with high new production and low export. *Journal of Plankton Research*, *38*(2), 348–365. https://doi.org/10.1093/plankt/fbv097

Teague, W. J., Jacobs, G. A., Ko, D. S., Tang, T. Y., Chang, K. I., & Suk, M. S. (2003). Connectivity of the Taiwan, Cheju, and Korea straits. *Continental Shelf Research*, *23*(1), 63–77. https://doi.org/10.1016/S0278-4343(02)00150-4

Umezawa, Y., Yamaguchi, A., Ishizaka, J., Hasegawa, T., Yoshimizu, C., Tayasu, I., et al. (2014). Seasonal shifts in the contributions of the Changjiang River and the Kuroshio current to nitrate dynamics in the continental shelf of the northern East China Sea based on a nitrate dual isotopic composition approach. *Biogeosciences*, *11*(4), 1297–1317. https://doi.org/10.5194/bg-11-1297-2014

Wang, H., Dai, M., Liu, J., Kao, S. J., Zhang, C., Cai, W. J., et al. (2016). Eutrophication-driven hypoxia in the East China Sea off the Changjiang Estuary. *Environmental Science & Technology*, *50*(5), 2255–2263. https://doi.org/10.1021/acs.est.5b06211

Wang, Y., Guo, X., Zhao, L., & Zhang, J. (2019). Seasonal variations in nutrients and biogenic particles in the upper and lower layers of East China Sea Shelf and their export to adjacent seas. *Progress in Oceanography*, *176*, 102138. https://doi.org/10.1016/j.pocean.2019.102138

Wu, C. R., Hsin, Y. C., Chiang, T. L., Lin, Y. F., & Tsui, I. F. (2014). Seasonal and interannual changes of the Kuroshio intrusion onto the East China Sea Shelf. *Journal of Geophysical Research: Oceans*, *119*(8), 5039–5051. https://doi.org/10.1002/2013JC009748

Xu, L., Yang, D., Benthuysen, J. A., & Yin, B. (2018). Key dynamical factors driving the Kuroshio subsurface water to reach the Zhejiang coastal area. *Journal of Geophysical Research: Oceans*, *123*(12), 9061–9081. https://doi.org/10.1029/2018JC014219

Yang, D., Yin, B., Hou, Y., Sun, S., Yu, Z., Song, J., et al. (2017). Research progress on the pathways of Kuroshio intrusion onto the East China Sea shelf and its impacts. *Oceanologia et Limnologia Sinica*, *48*(6), 1196–1207. (in Chinese). https://doi.org/10.11693/hyhz20170900223

Yang, D., Yin, B., Liu, Z., Bai, T., Qi, J., & Chen, H. (2012). Numerical study on the pattern and origins of Kuroshio branches in the bottom water of southern East China Sea in summer. *Journal of Geophysical Research*, *117*(C2). https://doi.org/10.1029/2011JC007528

Yang, D., Yin, B., Liu, Z., & Feng, X. (2011). Numerical study of the ocean circulation on the East China Sea shelf and a Kuroshio bottom branch northeast of Taiwan in summer. *Journal of Geophysical Research*, *116*(C5), C05015. https://doi.org/10.1029/2010JC006777

Zhang, J., Guo, X., & Zhao, L. (2019). Tracing external sources of nutrients in the East China Sea and evaluating their contributions to primary production. *Progress in Oceanography*, *176*, 102122. https://doi.org/10.1016/j.pocean.2019.102122

Zhang, J., Guo, X., & Zhao, L. (2021). Budget of riverine nitrogen over the East China Sea shelf. *Environmental Pollution*, *289*, 117915. https://doi.org/10.1016/j.envpol.2021.117915

Zhang, J., Guo, X., Zhao, L., Miyazawa, Y., & Sun, Q. (2017). Water exchange across isobaths over the continental shelf of the East China Sea. *Journal of Physical Oceanography*, *47*(5), 1043–1060. https://doi.org/10.1175/JPO-D-16-0231.1

Zhang, J., Liu, S. M., Ren, J. L., Wu, Y., & Zhang, G. L. (2007). Nutrient gradients from the eutrophic Changjiang (Yangtze River) Estuary to the oligotrophic Kuroshio waters and re-evaluation of budgets for the East China Sea shelf. *Progress in Oceanography*, *74*(4), 449–478. https://doi.org/10.1016/j.pocean.2007.04.019

Zhang, J., Zhu, L., Guo, X., Wang, Y., Feng, J., & Zhao, L. (2024). Export production in a continental shelf with multisource nutrient supply. *Frontiers in Marine Science*, *11*, 1338835. https://doi.org/10.3389/fmars.2024.1338835

Zhao, L., & Guo, X. (2011). Influence of cross-shelf water transport on nutrients and phytoplankton in the East China Sea: A model study. *Ocean Science*, *7*(1), 27–43. https://doi.org/10.5194/os-7-27-2011

Zhou, F., Xue, H., Huang, D., Xuan, J., Ni, X., Xiu, P., & Hao, Q. (2015). Cross-shelf exchange in the shelf of the East China Sea. *Journal of Geophysical Research: Oceans*, *120*(3), 1545–1572. https://doi.org/10.1002/2014JC010567

Zuo, J. L. (2018). *Analysis of nutrient transport from the kuroshio to the East China Sea and its controlling factors*. (Doctoral dissertation). University of Chinese Academy of Sciences. (in Chinese).

References From the Supporting Information

Hao, Q., Chai, F., Xiu, P., Bai, Y., Chen, J., Liu, C., et al. (2019). Spatial and temporal variation in chlorophyll a concentration in the Eastern China Seas based on a locally modified satellite dataset. *Estuarine, Coastal and Shelf Science*, *220*, 220–231. https://doi.org/10.1016/j.ecss.2019.01.004

Wang, W., Yu, Z., Song, X., Wu, Z., Yuan, Y., Zhou, P., & Cao, X. (2016). The effect of Kuroshio current on nitrate dynamics in the southern East China Sea revealed by nitrate isotopic composition. *Journal of Geophysical Research: Oceans*, *121*(9), 7073–7087. https://doi.org/10.1002/2016JC011882

Xu, L. J. (2019). *The intrusion mechanism and ecological effects of Kuroshio subsurface water in the Changjiang Estuary and its adjacent sea area*. (Doctoral dissertation). University of Chinese Academy of Sciences. (in Chinese).

Yang, D., Yin, B., Sun, J., & Zhang, Y. (2013). Numerical study on the origins and the forcing mechanism of the phosphate in upwelling areas off the Coast of Zhejiang province, China in summer. *Journal of Marine Systems*, *123*, 1–18. https://doi.org/10.1016/j.jmarsys.2013.04.002